Multi-Line Geometry of Qubit–Qutrit and Higher-Order Pauli Operators

Michel Planat · Anne-Céline Baboin · Metod Saniga

Abstract The commutation relations of the generalized Pauli operators of a qubit–qutrit system are discussed in the newly established graph-theoretic and finite-geometrical settings. The dual of the Pauli graph of this system is found to be isomorphic to the projective line over the product ring $\mathcal{Z}_2 \times \mathcal{Z}_3$. A "peculiar" feature in comparison with two-qubits is that two distinct points/operators can be joined by more than one line. The multi-line property is shown to be also present in the graphs/geometries characterizing two-qutrit and three-qubit Pauli operators' space and surmised to be exhibited by any other higher-level quantum system.

Keywords Generalized Pauli operators · Pauli graphs · Finite projective geometries

1 Introduction

Although being central to topics such as the derivation of complete sets of mutually un-biased bases [1, 2], or to an in depth understanding of quantum entanglement [3, 4], the commutation relations between the generalized Pauli operators of finite-dimensional quantum systems are still not well understood. Recently, considerable progress has been made in this respect by employing finite geometries such as finite projective lines [4, 5], generalized

M. Planat (✉) · A.-C. Baboin
Institut FEMTO-ST, CNRS, Département LPMO, 32 Avenue de l'Observatoire, 25044 Besançon, France
e-mail: michel.planat@femto-st.fr

M. Saniga
Astronomical Institute, Slovak Academy of Sciences, 05960 Tatranská Lomnica, Slovak Republic
e-mail: msaniga@astro.sk

quadrangles [6–8] and polar spaces [9, 10] to treat dimensions $d = 2^N$ and, most recently [7, 11], also the case of $d = 9$. In this paper, after introducing the basic notation about generalized Pauli operators and Pauli graphs and brief recalling the established results, we will first have a look at the smallest composite dimension, $d = 6$, as this is the first case where we expect to find serious departures from what is known about Hilbert spaces whose dimension is a power of a prime. We shall, indeed, find that the finite geometry here is more intricate, exhibiting more than one line sharing two distinct points. In light of this finding, we then revisit the $d = 3^2$ case and, finally, briefly address the case of $d = 2^3$.

A complete orthonormal set of operators in a p-dimensional Hilbert space (p a prime number) is of cardinality of $p^2 - 1$. These operators can be derived from the *shift* and *clock* operators X and Z

$$X|n\rangle = |n+1\rangle, \qquad Z|n\rangle = \omega_p^n |n\rangle \quad \text{with } \omega_p = \exp(2i\pi/p), \qquad (1)$$

as follows [1, 3],

$$\begin{aligned} \{Z^k\}, \quad & k = 1, \ldots, p-1, \\ \{(XZ^m)^k\}, \quad & k = 1, \ldots, p-1, \ m = 0, \ldots, p-1, \end{aligned} \qquad (2)$$

and grouped together into $p+1$ disjoint classes, each comprising $p-1$ pairwise commuting members. The common eigenstates of distinct classes form different sets of mutually unbiased bases [1, 3]. As a result, such sets of mutually unbiased bases are complete for Hilbert spaces of the corresponding dimensions.

The simplest ($p = 2$) case corresponds to qubits. The orthonormal set comprises the standard Pauli matrices $\sigma_i = (I_2, \sigma_x, \sigma_y, \sigma_z)$, $i \in \{0, 1, 2, 3\}$, where $I_2 = \begin{pmatrix} 1 & 0 \\ 0 & 1 \end{pmatrix}$, $\sigma_x = \begin{pmatrix} 0 & 1 \\ 1 & 0 \end{pmatrix}$, $\sigma_z = \begin{pmatrix} 1 & 0 \\ 0 & -1 \end{pmatrix}$ and $\sigma_y = i\sigma_x\sigma_z$. In the next case, $p = 3$, one gets $\sigma_j = \{I_3, Z, X, Y, V, Z^2, X^2, Y^2, V^2\}$, $j \in \{0, \ldots, 8\}$, where I_3 is the 3×3 unit matrix, $Z = \begin{pmatrix} 1 & 0 & 0 \\ 0 & \omega & 0 \\ 0 & 0 & \omega^2 \end{pmatrix}$, $X = \begin{pmatrix} 0 & 0 & 1 \\ 1 & 0 & 0 \\ 0 & 1 & 0 \end{pmatrix}$, $Y = XZ$, $V = XZ^2$ and $\omega = \exp(2i\pi/3)$. The implementation of this procedure for an arbitrary prime p is then straightforward. Going to Hilbert spaces of prime-power dimensions $d = p^N$, $N \geq 2$, the $(d^2 - 1)$ generalized Pauli operators are similarly partitioned into $(d + 1)$ disjoint sets, each one composed of a maximum set of $(d - 1)$ mutually commuting members.

In our graph-geometrical approach [4–7, 9], the generalized Pauli operators are identified with the points/vertices and maximum mutually commuting members of them with the edges/lines (or subspaces of higher dimensions) of a specific Pauli graph/finite incidence geometry so that the structure of the operators' space can fully be inferred from the properties of the Pauli graph/finite geometry in question. It has been found that the operators' space characterizing two-qubits is isomorphic to the generalized quadrangle of order two [6, 7] and that N-qubits ($N > 2$) are intimately related with symplectic polar spaces of rank N and order two [9]. A crucial role in this discovery turned out to be the concept of projective lines defined over rings [12], as the generalized quadrangle of order two is embedded as a sub-geometry in the distinguished projective line defined over the full two-by-two matrix ring with coefficients in $\mathcal{Z}_2$ [6]. When analyzing in a similar fashion two-qutrit ($d = 3^2$) case [7, 11], it turned out to be convenient to pass to the *dual* of the Pauli graph, i.e., to the graph whose vertices are represented by the *maximum commuting subsets* of the operators, two vertices being adjacent if the corresponding maximum sets have an operator in common. This move is also a fruitful and necessary one when addressing properly the simplest composite ($d = 6$) case, which is the subject of the next section.

2 The "Multi-Line" Geometry of a Qubit–Qutrit

For the sextic ($d = 6$) systems, one has $6^2 - 1 = 35$ generalized Pauli operators[1]

$$\Sigma_6^{(i,j)} = \sigma_i \otimes \sigma_j, \quad i \in \{0, \ldots, 3\}, \ j \in \{0, \ldots, 8\}, \ (i, j) \neq (0, 0), \tag{3}$$

which can be conveniently labelled as follows: $1 = I_2 \otimes \sigma_1, 2 = I_2 \otimes \sigma_2, \ldots, 8 = I_2 \otimes \sigma_8$, $a = \sigma_z \otimes I_3, 9 = \sigma_z \otimes \sigma_1, \ldots, b = \sigma_x \otimes I_3, 17 = \sigma_x \otimes \sigma_1, \ldots, c = \sigma_y \otimes I_3, \ldots, 32 = \sigma_y \otimes \sigma_8$. Joining two distinct mutually commuting operators by an edge, one obtains the corresponding Pauli graph $\mathcal{P}_6$. It is straightforward to derive twelve maximum commuting sets of operators,

$$L_1 = \{1, 5, a, 9, 13\}, \qquad L_2 = \{2, 6, a, 10, 14\},$$
$$L_3 = \{3, 7, a, 11, 15\}, \qquad L_4 = \{4, 8, a, 12, 16\},$$
$$M_1 = \{1, 5, b, 17, 21\}, \qquad M_2 = \{2, 6, b, 18, 22\},$$
$$M_3 = \{3, 7, b, 19, 23\}, \qquad M_4 = \{4, 8, b, 19, 24\},$$
$$N_1 = \{1, 5, c, 25, 29\}, \qquad N_2 = \{2, 6, c, 26, 30\},$$
$$N_3 = \{3, 7, c, 27, 31\}, \qquad N_4 = \{4, 8, c, 28, 32\},$$

which are regarded as lines of the associated finite geometry. Then, considering these lines as the vertices of the dual graph, $\mathcal{W}_6$, with an edge joining two vertices representing concurrent lines, we arrive at a grid-like graph shown in Fig. 1, right. This graph corresponds to $L[K(4, 3)]$, i.e., to the line graph of the bipartite graph $K(4, 3)$; it is a regular graph with
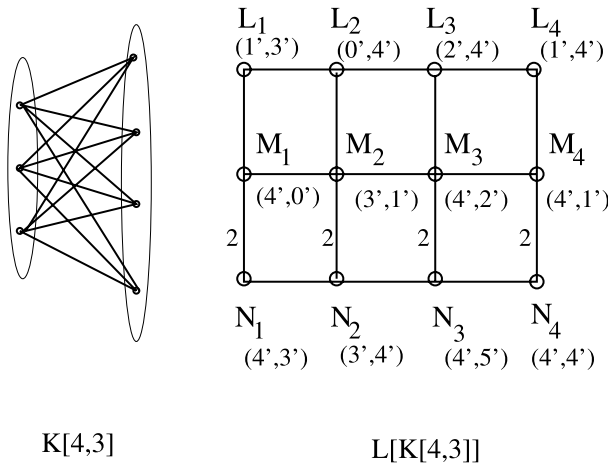

K[4,3]   L[K[4,3]]

Fig. 1 The graph $\mathcal{W}_6$, the dual of the Pauli graph $\mathcal{P}_6$, as the line graph of the complete bipartite graph $K[4, 3]$. The mutually unbiased bases correspond to the lines of the Pauli graph $\mathcal{P}_6$ which are not concurrent, i.e., to the vertices of $\mathcal{W}_6$ which are not adjacent. Lines L_i (as well as M_i and N_i) mutually intersect at a single point, whereas L_i and M_i (as well as L_i and N_i and M_i and N_i) have two points in common; this means that the adjacency in $\mathcal{W}_6$ is of two different "weights" ("1" and "2", the latter explicitly indicated). This 3×4 grid can also be regarded as the projective line over the ring $\mathcal{Z}_2 \times \mathcal{Z}_3$

---

[1]It is obvious that the geometry of a qutrit–qubit system is isomorphic to that of the qubit–qutrit case.

Fig. 2 A schematic sketch of the point-set structure of $\mathcal{S}_1 = \{L_1, M_1, N_1\}$
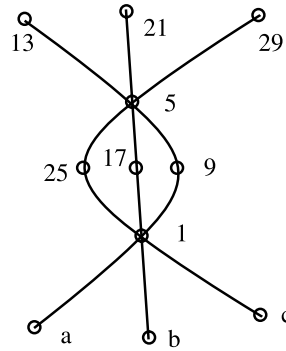
spectrum $\{-2^6, 1^3, 2^2, 5\}$. Mutually unbiased bases correspond to mutually disjoint lines and, hence, non-adjacent vertices of $\mathcal{W}_6$; from Fig. 1, right, it is readily seen that a maximum of three of them arise, as expected [15]. It is also worth mentioning that $\mathcal{W}_6$ can be regarded the projective line over the product ring $\mathcal{Z}_2 \times \mathcal{Z}_3 \cong Z_6$, where the term "adjacent" means "neighbor" (see Appendix for more details).

Returning back to $\mathcal{P}_6$ we can show that the associated geometry resembles to some extent that of a finite (0, 1)-geometry, i.e., the point-line incidence structure where (i) two distinct points are contained in at most one line, and where (ii) given a line and a point not on the line (*aka* an anti-flag), there exists either zero or one line through the point that intersect the line in question [8, 13]. For although we saw that our geometry is endowed with "multi-lines" (i.e., lines sharing more than one point) and so violates the first axiom of a (0, 1)-geometry, we still find that the connection number for each anti-flag is either zero or one. Hence, we can define an analogue of a geometric hyperplane (see, e.g., [14]) as a subset of points of our $\mathcal{P}_6$ geometry such that whenever its two points lie on a line then the entire line lies in the subset. Then we readily verify that the sets of points located on the following four triples of lines

$$\mathcal{S}_i = \{L_i, M_i, N_i\}, \quad i = 1, 2, 3, 4 \tag{4}$$

represent each a "geometric hyperplane" of our geometry, as illustrated in Fig. 2 for $\mathcal{S}_1$. The three lines of $\mathcal{S}_i$ intersects at two points and the connection number for any of its anti-flags is one.

3 The "Multi-Line" Geometry Behind Two-Qutrits

For the two-qutrit system ($d = 9$) one has the $9^2 - 1 = 80$ generalized Pauli operators

$$\Sigma_9^{(i,j)} = \sigma_i \otimes \sigma_j, \quad i \in \{0, \dots, 8\}, \ j \in \{0, \dots, 8\} \text{ and } (i, j) \neq (0, 0) \tag{5}$$

which can be labelled as follows: $1 = I_3 \otimes \sigma_1, 2 = I_3 \otimes \sigma_2, \dots, 8 = I_3 \otimes \sigma_8, a = \sigma_1 \otimes I_3, 9 = \sigma_1 \otimes \sigma_1, \dots, b = \sigma_2 \otimes I_3, 17 = \sigma_2 \otimes \sigma_1, \dots, c = \sigma_3 \otimes I_3, \dots, h = \sigma_8 \otimes I_3, \dots, 72 = \sigma_8 \otimes \sigma_8$. The associated Pauli graph $\mathcal{P}_9$ is regular, of degree 25, and its spectrum is $\{-7^{15}, -1^{40}, 5^{24}, 25\}$ [11]. It is a straightforward, but rather cumbersome, task to

derive the following 40 maximum commuting sets of operators

$$
\begin{array}{ll}
L_1 = \{1, 5, a, 9, 13, e, 41, 45\}, & L_2 = \{2, 6, a, 10, 14, e, 42, 46\}, \\
L_3 = \{3, 7, a, 11, 15, e, 43, 47\}, & L_4 = \{4, 8, a, 12, 16, e, 44, 48\}, \\
M_1 = \{1, 5, b, 17, 21, f, 49, 53\}, & M_2 = \{2, 6, b, 18, 22, f, 50, 54\}, \\
M_3 = \{3, 7, b, 19, 23, f, 51, 55\}, & M_4 = \{4, 8, b, 20, 24, f, 52, 56\}, \\
N_1 = \{1, 5, c, 25, 29, g, 57, 61\}, & N_2 = \{2, 6, c, 26, 30, g, 58, 62\}, \\
N_3 = \{3, 7, c, 27, 31, g, 59, 63\}, & N_4 = \{4, 8, c, 28, 32, g, 60, 64\}, \\
P_1 = \{1, 5, d, 33, 37, h, 65, 69\}, & P_2 = \{2, 6, d, 34, 38, h, 66, 70\}, \\
P_3 = \{3, 7, d, 35, 39, h, 67, 71\}, & P_4 = \{4, 8, d, 36, 40, h, 68, 72\}, \\
X_1 = \{9, 22, 32, 39, 45, 50, 60, 67\}, & X_2 = \{10, 17, 27, 40, 46, 53, 63, 68\}, \\
X_3 = \{11, 20, 30, 33, 47, 56, 58, 69\}, & X_4 = \{12, 23, 25, 34, 48, 51, 61, 70\}, \\
X_5 = \{13, 18, 28, 35, 41, 54, 64, 71\}, & X_6 = \{14, 21, 31, 36, 42, 49, 59, 72\}, \\
X_7 = \{15, 24, 26, 37, 43, 52, 62, 65\}, & X_8 = \{16, 19, 29, 38, 44, 55, 57, 66\}, \\
Y_1 = \{9, 23, 30, 40, 45, 51, 58, 68\}, & Y_2 = \{10, 19, 32, 33, 46, 55, 60, 69\}, \\
Y_3 = \{11, 22, 25, 36, 47, 50, 61, 72\}, & Y_4 = \{12, 17, 26, 39, 48, 53, 62, 67\}, \\
Y_5 = \{13, 20, 27, 34, 41, 56, 63, 70\}, & Y_6 = \{14, 23, 28, 37, 42, 51, 64, 65\}, \\
Y_7 = \{15, 18, 29, 40, 43, 54, 57, 68\}, & Y_8 = \{16, 21, 30, 35, 44, 49, 58, 71\}, \\
Z_1 = \{9, 24, 31, 38, 45, 52, 59, 66\}, & Z_2 = \{10, 24, 25, 35, 46, 52, 61, 71\}, \\
Z_3 = \{11, 17, 28, 38, 47, 53, 64, 66\}, & Z_4 = \{12, 18, 31, 33, 48, 54, 59, 69\}, \\
Z_5 = \{13, 19, 26, 36, 41, 55, 62, 72\}, & Z_6 = \{14, 20, 29, 39, 42, 56, 57, 67\}, \\
Z_7 = \{15, 21, 32, 34, 43, 49, 60, 70\}, & Z_8 = \{16, 22, 27, 37, 44, 50, 63, 65\}.
\end{array}
\tag{6}
$$

From there we find that the dual graph $\mathcal{W}_9$ consists of 40 vertices and has spectrum $\{-4^{15}, 2^{24}, 12\}$, which are the characteristics identical with those of the generalized quadrangle of order three formed by the points and lines of a parabolic quadric $Q(4, 3)$ in $PG(4, 3)$ [8]. The quadrangle $Q(4, 3)$, like its two-qubit counterpart, exhibits all the three kinds of geometric hyperplanes, a grid (of order (3,1)), an ovoid, and a perp-set (see, e.g., [14]), and these three kinds of subsets are all indeed found to sit inside the finite geometry associated with $\mathcal{W}_9$ [11].

A grid of $\mathcal{W}_9$ is shown in Fig. 3a. The subsets of points lying on the following quadruples of lines

$$
\mathcal{S}_i = \{L_i, M_i, N_i, P_i\}, \quad i = 1, 2, 3, 4,
\tag{7}
$$

then represent "multi-line hyperplanes" in the geometry associated with $\mathcal{P}_9$, as depicted in Fig. 3b; the "multi-line hyperplane" corresponding to the grid as a whole is obtained by taking all the four copies $\mathcal{S}_i$, having the eight reference points $a, b, \dots, h$ in common. Figure 4 shows an ovoid of $\mathcal{W}_9$ (a) and its counterpart in the $\mathcal{P}_9$ geometry (b); the bases associated with the operators on any two distinct lines of this set are mutually unbiased and, when taken together, they thus form a complete set for this dimension. Finally, Fig. 5 gives an example of a perp-set of $\mathcal{W}_9$ (a) together with the detailed structure of its "multi-line" counterpart in $\mathcal{P}_9$ (b).

Fig. 3 **a** An example of a grid in $\mathcal{W}_9$; each edge is of the same weight as every pair of concurrent lines intersect at two points as indicated. **b** A set of four lines L_i, M_i, N_i, P_i form a "multi-line" subset of the geometry associated with $\mathcal{P}_9$, here illustrated for $i = 1$

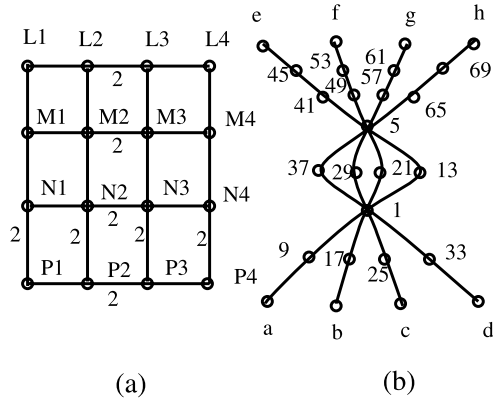

(a)   (b)

Fig. 4 **a** An ovoid of $\mathcal{W}_9$, i.e., a set of ten pairwise non-collinear points, and **b** its image in the geometry of $\mathcal{P}_9$, i.e., a set of ten pairwise disjoint (or parallel) lines

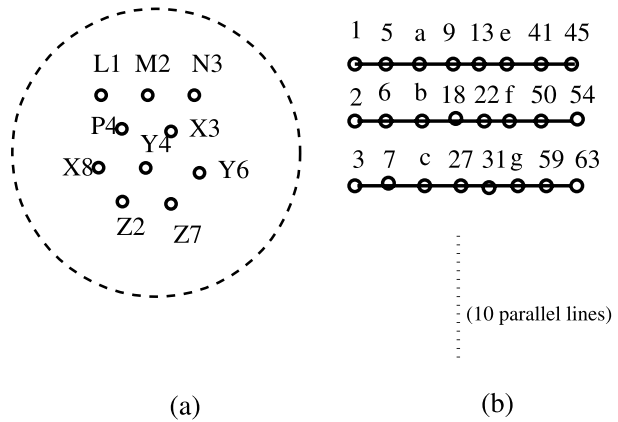(a)   (b)

Fig. 5 **a** One of the perp-sets in $\mathcal{W}_9$, and **b** its dual "multi-line" twin; in the latter case, the structure of only one of the four "multi-line" subsets is shown in full detail
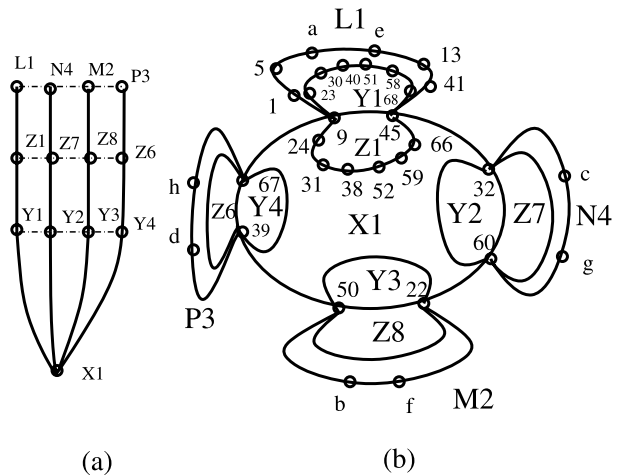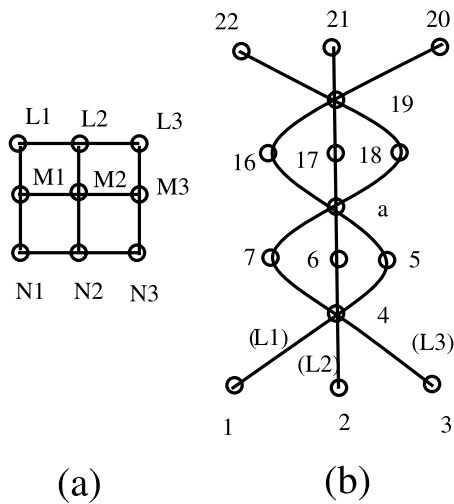

(a)   (b)

Fig. 6 **a** A 3×3 grid in the $\mathcal{W}_8$ representation of the three-qubit system with adjacency of weight three, and **b** its generic part unveiled in the $\mathcal{P}_8$ perspective. Seven observables are shared by the triple of lines in a row of the square, but only three by the triple of lines in a column

(a)   (b)

4 Hints About "Multi-Line" Configurations Pertinent to Three-Qubits

It is worth observing that whereas in the case of two-qubits there exists a perfect duality between the operators (points) and maximum commuting (sub)sets of them (lines) [6, 7], this property is lost when we pass to higher level quantum systems; thus, as we have seen, in the qubit–qutrit case we have 35 operators but only 12 lines, whereas two-qutrits give 80 operators and 40 lines. We surmise that it is this loss of duality which enables the emergence of "multi-line" objects in the corresponding finite geometries.

To partly justify this surmise, we will briefly address the case of three-qubits. The $4^3 - 1 = 63$ tensor products of the classical Pauli matrices $\sigma_i \otimes \sigma_j \otimes \sigma_k$, $[i, j, k = 0, 1, 2, 3, (i, j, k) \neq (0, 0, 0)]$ form the vertices and their commuting pairs the edges of the strongly regular graph, $\mathcal{P}_8$, of degree 30 and spectrum $\{-5^{27}, 3^{35}, 30\}$. Employing the same strategy for labelling the operators as in the preceding sections, i.e., $1 = I_2 \otimes I_2 \otimes \sigma_1, 2 = I_2 \otimes I_2 \otimes \sigma_2, \ldots, 15 = I_2 \otimes \sigma_3 \otimes \sigma_3, a = \sigma_1 \otimes I_2 \otimes I_2$, etc., one finds out that the lines of the associated geometry, of cardinality seven each, allow indeed the existence "multi-line hyperplanes." A portion of one of them is shown in Fig. 6, fully in the $\mathcal{W}_8$ (a) and partially in the $\mathcal{P}_8$ (b) representation; the 3×3 grid can be regarded as a dual analogue of the classical Mermin square in the space of observables of two-qubits, which is a crucial element in the proof of the Kochen–Specker theorem in dimension four [16].

5 Conclusion

Given a finite-dimensional quantum system, the set of corresponding generalized Pauli operators and the set of maximum commuting subsets of them can be viewed as a point-line incidence geometry in a dual way; either regarding the operators as the points and the maximum commuting subsets as the lines, or vice versa. In the two-qubit case, the two pictures have been found to be isomorphic to each other thanks to the fact that the underlying geometry, a finite generalized quadrangle of order two, is a self-dual object [6, 7]. This self-duality, however, seems to disappear as we go to higher-dimensional Hilbert spaces. An intriguing symptom of this broken symmetry is that in one of the two representations we encounter

lines sharing more than one point in common, as illustrated here in detail for the cases of dimension six, nine and eight. We surmise that this holds true for any finite-dimensional quantum system except for two-qubits.

Appendix

The concept of a projective line defined over a (finite) ring [12, 17] turned out of great importance in discovering the relevance of finite projective geometries for a deeper understanding of finite-dimensional quantum systems. This started with recognition of the projective line over $\mathcal{Z}_2 \times \mathcal{Z}_2$ behind a Mermin square of two-qubits [5], and followed by realization that the geometry of two-qubits is fully embedded within the line defined over the smallest 2×2 matrix ring, $\mathcal{Z}_2^{2\times2}$ [6]. Here we shall demonstrate that $\mathcal{W}_6$ is isomorphic to the projective line over the ring $\mathcal{Z}_2 \times \mathcal{Z}_3$.

Given an associative ring R with unity and $GL(2, R)$, the general linear group of invertible two-by-two matrices with entries in R, a pair (α, β) is called admissible over R if there exist $\gamma, \delta \in R$ such that $\left(\begin{smallmatrix} \alpha & \beta \\ \gamma & \delta \end{smallmatrix}\right) \in GL_2(R)$. The projective line over R is defined as the set of equivalence classes of ordered pairs $(\varrho\alpha, \varrho\beta)$, where ϱ is a unit of R and (α, β) admissible [17]. Such a line carries two non-trivial, mutually complementary relations of neighbor and distant. In particular, its two distinct points X: $(\varrho\alpha, \varrho\beta)$ and Y: $(\varrho\gamma, \varrho\delta)$ are called *neighbor* if $\left(\begin{smallmatrix} \alpha & \beta \\ \gamma & \delta \end{smallmatrix}\right) \notin GL_2(R)$ and *distant* otherwise. The structure of the line over a finite ring can be illustrated in terms of a graph whose vertices are the points of the line and edges join any two mutually neighbor points.

The elements of the ring $\mathcal{Z}_2 \times \mathcal{Z}_3 \cong Z_6$ can be taken in the form $0' = (0, 0)$, $1' = (0, 1)$, $2' = (0, 2)$, $3' = (1, 0)$, $4' = (1, 1)$ and $5' = (1, 2)$, where the first element in a pair belongs to $\mathcal{Z}_2$ and the second to $\mathcal{Z}_3$. Addition and multiplication is carried out component-wise (Table 1) and one finds that the ring contains four zero-divisors $(0', 1', 2', 3')$ and two units $(4'$ and $5')$. Employing the above-given definition, it follows that the corresponding projective line is endowed with twelve points out of which (i) eight are represented by pairs where at least one entry is a unit, (ii) two has both entries units, and (iii) two have both entries zero divisors, namely

(i) $(4', 0'), (4', 1'), (4', 2'), (4', 3'), (0', 4'), (1', 4'), (2', 4'), (3', 4')$.
(ii) $(4', 4'), (4', 5')$.
(iii) $(1', 3'), (3', 1')$.

It is an easy exercise to check that the graph of the line is identical to that shown in Fig. 1, right (see also [18]), which implies its isomorphism to $\mathcal{W}_6$.

Table 1 Addition (*left*) and multiplication (*right*) in $\mathcal{Z}_2 \times \mathcal{Z}_3$

+	$0'$	$1'$	$2'$	$3'$	$4'$	$5'$		$\times$	$0'$	$1'$	$2'$	$3'$	$4'$	$5'$
$0'$	$0'$	$1'$	$2'$	$3'$	$4'$	$5'$		$0'$	$0'$	$0'$	$0'$	$0'$	$0'$	$0'$
$1'$	$1'$	$2'$	$0'$	$4'$	$5'$	$3'$		$1'$	$0'$	$1'$	$2'$	$0'$	$1'$	$2'$
$2'$	$2'$	$0'$	$1'$	$5'$	$3'$	$4'$		$2'$	$0'$	$2'$	$1'$	$0'$	$2'$	$1'$
$3'$	$3'$	$4'$	$5'$	$0'$	$1'$	$2'$		$3'$	$0'$	$0'$	$0'$	$3'$	$3'$	$3'$
$4'$	$4'$	$5'$	$3'$	$1'$	$2'$	$0'$		$4'$	$0'$	$1'$	$2'$	$3'$	$4'$	$5'$
$5'$	$5'$	$3'$	$4'$	$2'$	$0'$	$1'$		$5'$	$0'$	$2'$	$1'$	$3'$	$5'$	$4'$

References

1. Bandyopadhyay, S., Boykin, P.O., Roychowdhury, V., Vatan, F.: A new proof for the existence of mutu-
   ally unbiased bases. Algorithmica **34**, 512–528 (2002)
2. Planat, M., Rosu, H.C., Perrine, S.: A survey of finite algebraic geometrical structures underlying mutu-
   ally unbiased measurements. Found. Phys. **36**, 1662–1680 (2006)
3. Klimov, A.B., Sanchez-Soto, L.L., de Guise, H.: Multicomplementary operators via finite Fourier trans-
   form. J. Phys. A **38**, 2747–2760 (2005)
4. Planat, M., Saniga, M., Kibler, M.: Quantum entanglement and projective ring geometry. SIGMA **2**,
   Paper 066 (2006)
5. Saniga, M., Planat, M.: Projective line over the finite quotient ring $GF(2)[x]/\langle x^3 - x \rangle$ and quantum
   entanglement: the Mermin "magic" square/pentagram. Theor. Math. Phys. **151**, 625–631 (2007)
6. Saniga, M., Planat, M., Pracna, P.: Projective ring line encompassing two-qubits. Theor. Math. Phys.
   (2006, accepted). quant-ph/0611063
7. Planat, M., Saniga, M.: On the Pauli graphs of N-qubits. Quantum Int. Comput. **8**, 127–146 (2008)
8. Payne, S.E., Thas, J.A.: Finite Generalized Quadrangles. Pitman, Boston (1984)
9. Saniga, M., Planat, M.: Multiple qubits and symplectic polar spaces of order two. Adv. Stud. Theor.
   Phys. **1**, 1–4 (2007)
10. Thas, K.: Pauli operators of N-qubit Hilbert spaces and the Saniga–Planat conjecture. Chaos, Solitons
    Fractals (2007, to appear)
11. Planat, M., Saniga, M.: Pauli graph and finite projective lines/geometries. In: Opt. Optoelectron. SPIE
    Proceedings, vol. 6583 (2007)
12. Saniga, M., Planat, M., Kibler, M.R., Pracna, P.: A classification of the projective lines over small rings.
    Chaos, Solitons Fractals **33**, 1095–1102 (2007)
13. Batten, L.M.: Combinatorics of Finite Geometries, 2nd edn. Cambridge University Press, Cambridge
    (1997)
14. Saniga, M., Planat, M., Pracna, P., Havlicek, H.: The Veldkamp space of two-qubits. SIGMA **3**, Paper 075
    (2007)
15. Grassl, M.: Quantum designs: MUBs, SICPOVMs, and (a little bit) more. Preprint available at avalon.
    ira.uka.de/home/grassl/paper/CEQIP_QDesigns.pdf
16. Mermin, N.D.: Hidden variables and two theorems of John Bell. Rev. Mod. Phys. **65**, 803–815 (1993)
17. Blunck, A., Havlicek, H.: Projective representations I: Projective lines over a ring. Abh. Math. Semin.
    Univ. Hamb. **70**, 287–299 (2000)
18. Havlicek, H.: Divisible designs, Laguerre geometry, and beyond. Quaderni del Seminario Matematico
    di Brescia **11**, 1–63 (2006). A preprint available from http://www.geometrie.tuwien.ac.at/havlicek/dd-
    laguerre.pdf